Supplementary Data for McNally et al. “Killing by Type VI secretion drives clonal phase separation and the evolution of cooperation”.

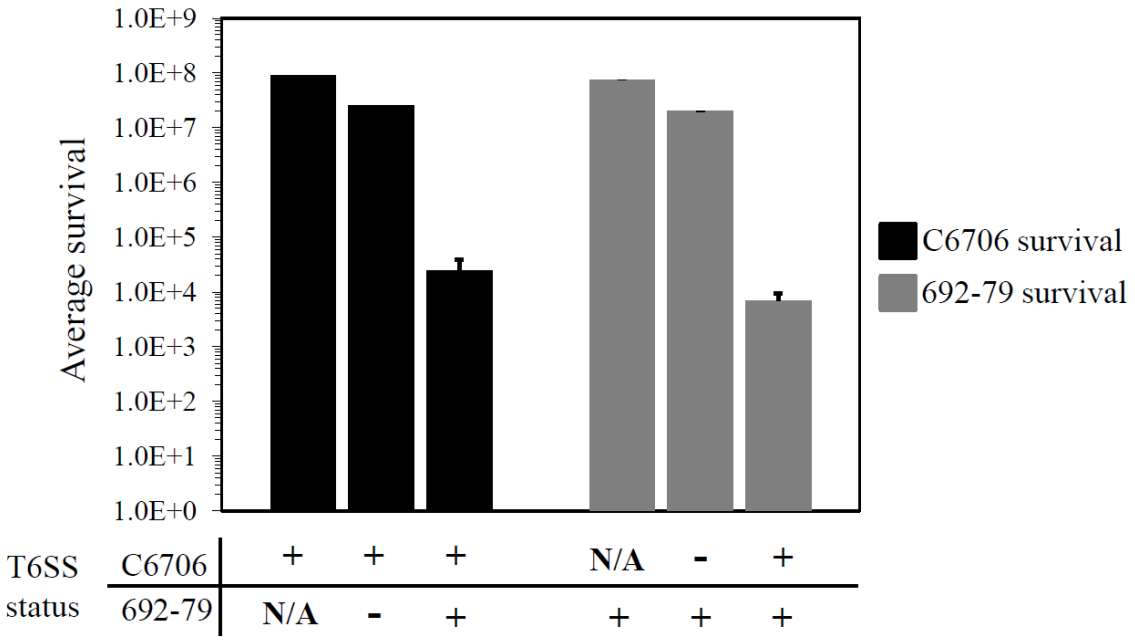

Figure S1. *Vibrio cholerae* strains C6706 and 692-79 are mutual killers. Spectinomycin resistant C6706 survival was measured after a 3 hour incubation on membrane filters on LB agar in a 1:10 ratio with LB broth[1], or liquid cultures of 692-79 T6SS$^-$ (Δ*vasK*), or 692-79 T6SS$^+$ strains and is represented by black bars. Kanamycin resistant 692-79 survival was measured similarly in a 1:10 ratio with LB broth, C6706 T6SS$^-$ (Δ*vask*), or C6706 T6SS$^+$ and is represented by gray bars. Sequencing confirms that these two strains have different sets of effector-immunity pairs, consistent with their ability to kill one another using T6S (Watve, Chande and Hammer, unpublished). Shown are average prey survival values ± one standard deviation after triplicate encounters. One representative experiment is shown of three performed.

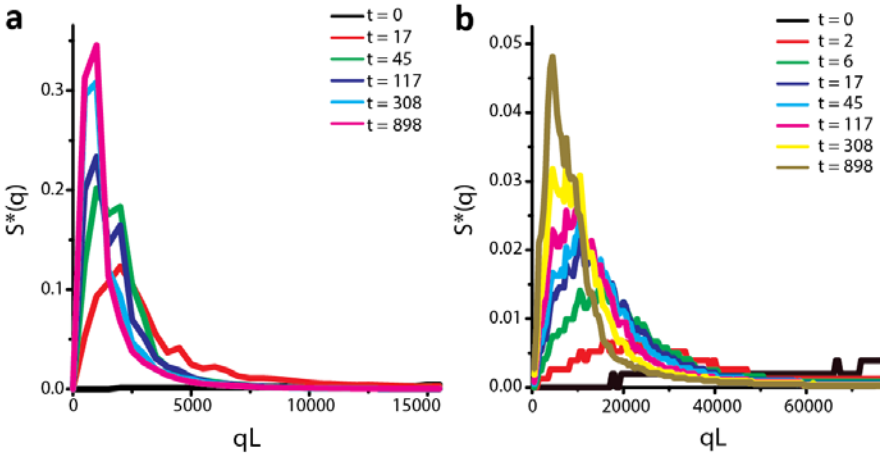

Figure S2. Structural analysis of additional models. The normalized static structure factor, *S*(q)*, is plotted at different times versus wavenumber, *q*, multiplied by cell size, *L*, for the PDE model with diffusion *d* = 0.01 (a) and the Ising model with Glauber spin flip dynamics on the square lattice (b). In both the PDE and Ising spin models, the peak in *S*(q)* increases in height and moves to smaller *q* values as time increases, just as was seen for the individual based model and experiments in Figure 2a and b, respectively.

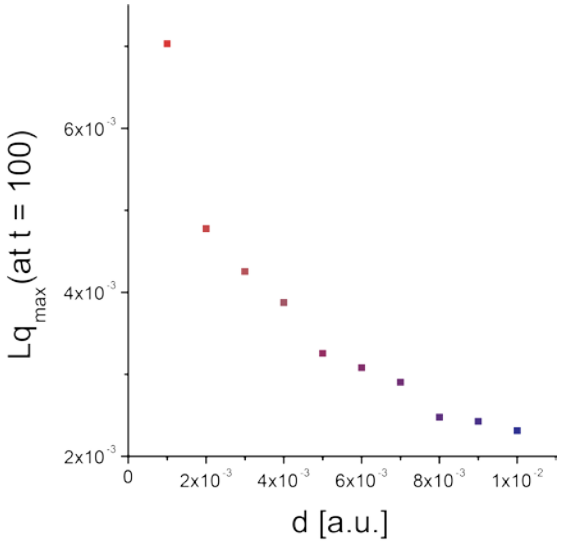

Figure S3. Cellular mobility speeds decomposition in the PDE model. For the PDE model, the value of q_{max} after 100 time steps, multiplied by cell size, *L*, is plotted vs. the rate of cellular mobility (random movement akin to diffusion), *d*. As *d* increases, the value of q_{max} decreases, indicating that the demixing process is further along.

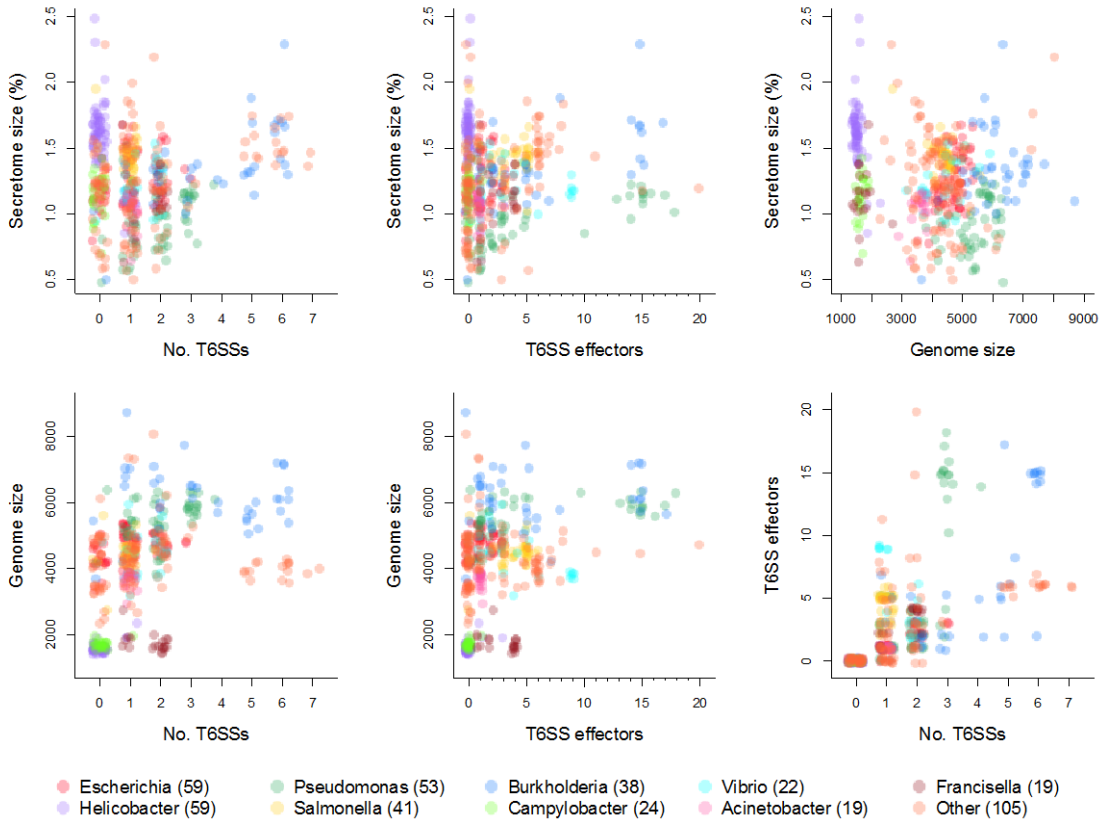

Figure S4. Scatterplots of raw data from comparative analysis. Shown are pairwise scatterplots of all data included in our comparative analysis. Colours indicate different genera as indicated in the legend.

Supplementary Movies

Supplementary Movie 1. Time-lapse of the individual based model. Both strains kill with equal probability. Each timestep, 5% of cells attempt to kill neighboring non-kin, and 5% of cells attempt to reproduce into an adjacent open patch.

Supplementary Movie 2. Time-lapse of the PDE model. Cellular mobility, d, is 0.001. Other parameter values are $r = 2$, $s = 2$, $\alpha_{AB} = 0.5$, $\alpha_{BA} = 0.5$.

Supplementary Movie 3. Time-lapse of the Ising spin model. Initial conditions correspond to infinite temperature, or completely random spins. Thermodynamic beta was set to unity and the eight nearest neighbors were considered. One generation is equivalent to an average of one spin-flip opportunity per site.

Supplementary Movie 4. Variation in cellular mobility (d) within the PDE model. Higher rates of mobility delay the formation of clonal patches, but increase the rate of phase separation.

Supplementary Movie 5. Public goods cooperation in the PDE model. In the leftmost panel cooperator frequency of 0 is represented by red and frequency of 1 by blue. In the center panel the concentration of public goods (produced by the cooperator) is indicated by intensity of yellow. In the rightmost panel the cell density is indicated by intensity of green. Parameter values are $r = 2$, $s = 2$, $\alpha_{AB} = 0.5$, $\alpha_{BA} = 0.5$, $d = 0.01$, $b = 1.9$, $c = 0.1$, $D = 0.1$, $\lambda = 100$, $\rho = 100$.

Supplementary Tables

Table S1: List of strains used in this study.

Vibrio cholerae strains	Genotype
C6706 red T6SS$^+$	Δ*vc1807*::p*tac-mKO* p*tac-qstR*
C6706 red T6SS$^-$	Δ*vc1807*::p*tac-mKO* p*tac-qstR* Δ*vasK*
C6706 green T6SS$^+$	Δ*vc1807*::p*tac-mTFP1* p*tac-qstR*
C6706 green T6SS$^-$	Δ*vc1807*::p*tac-mTFP1* p*tac-qstR* Δ*vasK*
692-79 red T6SS$^+$	*lacZ*::p*tac-mKO*
692-79 red T6SS$^-$	*lacZ*::p*tac-mKO* Δ*vasK*
692-79 green T6SS$^+$	*lacZ*::p*tac-mTFP1*
692-79 green T6SS$^-$	*lacZ*::p*tac-mTFP1* Δ*vasK*

Table S2: Effects of numbers of T6SSs and T6SS effectors on secretome size.

Fixed Terms	**Parameter Estimate**	**Lower 95% C.I.**	**Upper 95% C.I.**	**P_{MCMC}**
Intercept	–4.4661	–4.7097	–4.2588	**<0.0001**
No. T6SSs	0.0322	0.0085	0.0559	**0.0076**
T6SS effectors	0.0105	0.0014	0.0194	**0.0228**
Random Terms	**Variance**	**Lower 95% C.I.**	**Upper 95% C.I.**	
Phylogenetic variance	0.0833	0.0611	0.1096	NA
Residual variance	0.0006	0.0002	0.0014	NA

Table S3: Effect of number of T6SSs on secretome size.

Fixed Terms	**Parameter Estimate**	**Lower 95% C.I.**	**Upper 95% C.I.**	**P_{MCMC}**
Intercept	–4.4652	–4.717	–4.2313	**<0.0001**
No. T6SSs	0.0456	0.0252	0.0672	**<0.0001**
Random Terms	**Variance**	**Lower 95% C.I.**	**Upper 95% C.I.**	
Phylogenetic variance	0.0854	0.0606	0.1102	NA
Residual variance	0.0007	0.0002	0.0014	NA

Table S4: Effect of number of T6SS effectors on secretome size.

Fixed Terms	**Parameter Estimate**	**Lower 95% C.I.**	**Upper 95% C.I.**	**P_{MCMC}**
Intercept	–4.44223	–4.66215	–4.22636	**<0.0001**
T6SS effectors	0.0164	0.0084	0.0242	**<0.0001**
Random Terms	**Variance**	**Lower 95% C.I.**	**Upper 95% C.I.**	
Phylogenetic variance	0.085	0.0612	0.1102	NA
Residual variance	0.0007	0.0002	0.0015	NA

Table S5: Effects of numbers of T6SSs, T6SS effectors and genome size on secretome size.

Fixed Terms	**Parameter Estimate**	**Lower 95% C.I.**	**Upper 95% C.I.**	**P_{MCMC}**
Intercept	–4.2362	–5.4144	–3.0159	**<0.0001**
No. T6SSs	0.0326	0.008	0.0564	**0.01**
T6SS effectors	0.0106	0.0021	0.0204	**0.0256**
Log genome size	–0.0279	–0.1777	0.1133	0.7248
Random Terms	**Variance**	**Lower 95% C.I.**	**Upper 95% C.I.**	
Phylogenetic variance	0.0838	0.0582	0.1074	NA
Residual variance	0.0007	0.0001	0.0014	NA

Supplementary Equations

Supplementary Equations 1. Type 6 secretion in a PDE model.

Well-mixed environment

We will consider the interaction of two strains with different T6SS effector-immunity pairs so that each strain can kill the other strain upon cell-cell contact. For simplicity, we assume that both strains differ only in their T6SSs, having the same basal growth rate *r* and density dependent mortality rate *s*. We allow for asymmetric killing between the strains so that strain *A* kills strain *B* at rate α_{BA} and strain *B* kills strain *A* at rate α_{AB}. From these assumptions we can write the change in density of strains *A* and *B* in a well-mixed environment as

$$\begin{aligned} \frac{dA}{dt} &= A(r - s(A+B) - \alpha_{AB}B) \\ \frac{dB}{dt} &= B(r - s(A+B) - \alpha_{BA}A) \end{aligned} \tag{1}$$

There are four possible equilibria for this system: a bacteria-free equilibrium at $A = 0$, $B = 0$; two single-strain equilibria at $A = r/s$, $B = 0$ and $A = 0$, $B = r/s$; and a coexistence equilibrium with both strains present at $A = \alpha_{AB}r/(s(\alpha_{AB} + \alpha_{BA}) + \alpha_{AB}\alpha_{BA})$, $B = \alpha_{BA}r/(s(\alpha_{AB} + \alpha_{BA}) + \alpha_{AB}\alpha_{BA})$. Note that at the coexistence equilibrium the ratio of strain *A* to strain *B* simply depends on their relative rates of killing ($A/B = \alpha_{AB}/\alpha_{BA}$). Analysing the Jacobian (*J*) of the system around the equilibrium we can see that the bacteria-free equilibrium is unstable as long as $r > 0$ ($\mathrm{tr}(J) = 2r, |J| = r^2$), while the single strain equilibria are always stable for our assumption of positive rates of killing ($\mathrm{tr}(J) = -r(s + \alpha_{BA})/s$, $|J| = \alpha_{BA}r^2/s$ for $A = r/s$, $B = 0$, and $\mathrm{tr}(J) = -r(s + \alpha_{AB})/s$, $|J| = \alpha_{AB}r^2/s$ for $A = 0$, $B = r/s$). Analysing the coexistence equilibrium we can see that both the trace and the determinant at the equilibrium are strictly negative

$$\mathrm{tr}(J) = -\frac{\alpha_{AB}\alpha_{BA}rs}{s(\alpha_{AB}+\alpha_{BA})+\alpha_{AB}\alpha_{BA}}$$
$$|J| = -\frac{\alpha_{AB}\alpha_{BA}r^2}{s(\alpha_{AB}+\alpha_{BA})+\alpha_{AB}\alpha_{BA}} \quad (2)$$

meaning that this is a saddle node, and is hence unstable. This means that in a well-mixed environment killing by T6SS will always lead to one strain coming to dominate the environment, with the critical ratio of strains *A* to *B* at which *A* eventually dominates decided by its relative rate of killing (*A* dominates if $A/B > \alpha_{AB}/\alpha_{BA}$) and vice versa for domination by strain *B*.

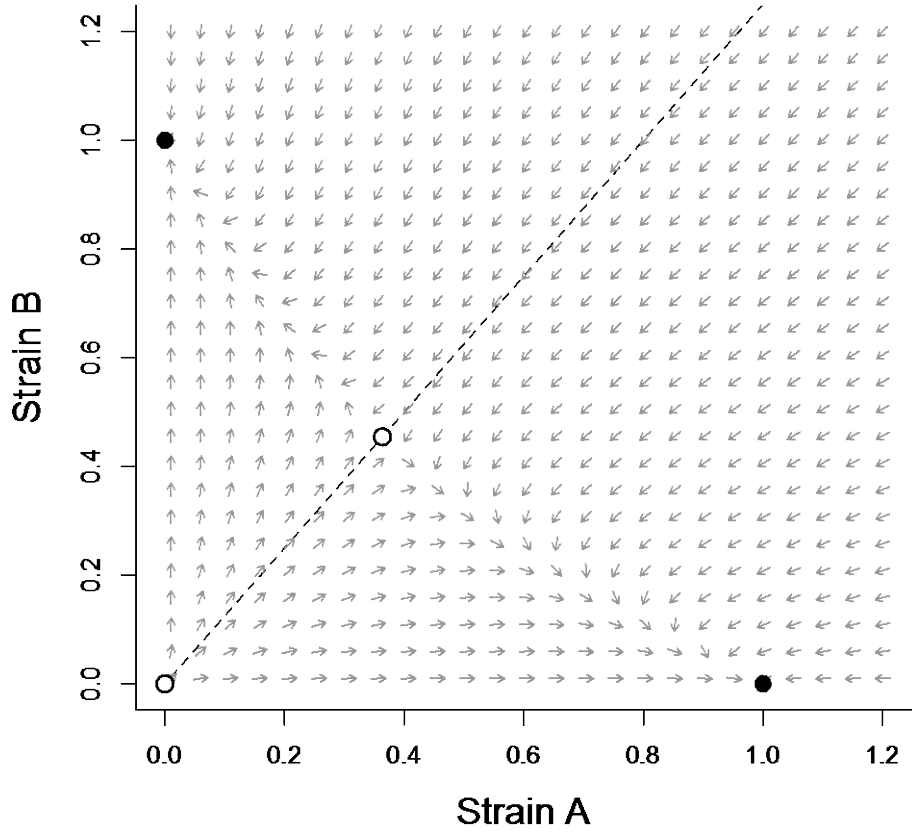

Figure SE1.1. Illustration of T6SS mediated dynamics in a well-mixed population. Arrows indicate the direction of the dynamics for any given combination of densities of strains *A* and *B*. Open circles indicate the unstable equilibria, while closed circles are stable equilibria. The dashed line indicates the critical ratio

of strains *A* and *B* dictating which stable equilibrium will be reached. Parameter values are $r = 2$, $s = 2$, $\alpha_{AB} = 0.8$ and $\alpha_{BA} = 1$. Note that for these parameter the basin of attraction for the equilibrium where *A* dominates ($A = r/s$, $B = 0$) is larger than the basin of attraction for the equilibrium where *B* dominates ($A = 0$, $B = r/s$) owing to *A*'s superior killing ability ($\alpha_{BA} > \alpha_{AB}$).

Spatially extended environment

In order to study the dynamics of strains with different T6SS effector-immunity pairs in a spatial environment we use the following system of partial differential equations

$$\begin{aligned} \frac{\partial A}{\partial t} &= A(r - s(A + B) - \alpha_{AB}B) + d\Delta A \\ \frac{\partial B}{\partial t} &= B(r - s(A + B) - \alpha_{BA}A) + d\Delta B \end{aligned} \tag{3}$$

The dynamics are given as before but with a Laplacian operator for the diffusion/dispersal of cells through space, where *d* is the dispersal/diffusion rate for both strains. We will first consider the stability of a homogenous coexistence equilibrium where the average densities of the strains are

$$\begin{aligned} A_0 &= \frac{\alpha_{AB} r}{s(\alpha_{AB} + \alpha_{BA}) + \alpha_{AB}\alpha_{BA}} \\ B_0 &= \frac{\alpha_{BA} r}{s(\alpha_{AB} + \alpha_{BA}) + \alpha_{AB}\alpha_{BA}} \end{aligned} \tag{4}$$

We will consider the effect of a fluctuation in the strain composition in one-dimensional space of the form

$$\begin{aligned} A(x) &= a \sin \beta x + A_0 \\ B(x) &= -a \sin \beta x + B_0 \end{aligned} \tag{5}$$

This fluctuation leads to a change in density of strain *A* at location *x* of $a \sin \beta x$ with a corresponding change of $-a \sin \beta x$ in the density of strain *B*, where *a* is the amplitude of the fluctuation (which e will

assume to be infinitesimally small) and β is the angular frequency. As we are concerned with changes in composition we will denote the density/volume fraction of strain *A* as $\varphi_A = A/(A+B)$ and using equation 3 the rate of change in the density fraction is

$$\frac{\partial \varphi_A}{\partial t} = \frac{B(d\Delta A - \alpha_{AB}AB) - A(d\Delta B - \alpha_{BA}AB)}{(A+B)^2} \tag{6}$$

Substituting in equations 4 and 5 we get

$$\begin{aligned}\frac{\partial \varphi_A}{\partial t} = -\frac{a\sin\beta x}{(\alpha_{AB}+\alpha_{BA})r^2}\Big(r\big(\beta^2 d(s(\alpha_{AB}+\alpha_{BA})+\alpha_{AB}\alpha_{BA})\big) \\ + a\sin\beta x\,(s(\alpha_{AB}+\alpha_{BA})+\alpha_{AB}\alpha_{BA})\big(r(\alpha_{AB}-\alpha_{BA}) \\ + a\sin\beta x\,(s(\alpha_{AB}+\alpha_{BA})+\alpha_{AB}\alpha_{BA})\big)\Big)\end{aligned} \tag{7}$$

For the compositions to diverge $\partial\varphi_A/\partial t$ must have the same sign as the fluctuation $\sin\beta x$, as this leads to *A* increase in frequency in regions of positive fluctuation and *B* to increase in frequency in regions of negative fluctuation. At any point of zero compositional fluctuation ($x = n\pi/\beta$, where $n \in \mathbb{Z}$), $\partial\varphi_A/\partial t = 0$ and this condition cannot be fulfilled. However, the condition for $\partial\varphi_A/\partial t$ and $\sin\beta x$ to have the same sign in a region of non-zero fluctuation ($x \neq n\pi/\beta$, where $n \in \mathbb{Z}$) is

$$\begin{aligned}\frac{\alpha_{AB}\alpha_{BA}r}{\alpha_{AB}\alpha_{BA}+s(\alpha_{AB}+\alpha_{BA})} \\ - \frac{a\sin\beta x\,(r(\alpha_{AB}-\alpha_{BA})+a\sin\beta x(s(\alpha_{AB}+\alpha_{BA})+\alpha_{AB}\alpha_{BA}))}{r} \\ > d\beta^2\end{aligned} \tag{8}$$

Assuming that the amplitude of the compositional fluctuation is infinitesimally small ($a \to 0$), inequality 8 simplifies to

$$\frac{\alpha_{AB}\alpha_{BA}r}{\alpha_{AB}\alpha_{BA}+s(\alpha_{AB}+\alpha_{BA})} > d\beta^2 \tag{9}$$

Therefore, the strain compositions will diverge, with *A* increasingly dominating in regions of positive compositional fluctuation and *B* coming to dominate in regions of negative compositional fluctuation, if the fluctuations occur on a sufficiently wide scale relative to bacterial dispersal/diffusion (i.e. sufficiently low *d* and/or β). It is also worth noting that this condition is more easily satisfied for higher rates of killing by both strains (higher α_{AB} and α_{AB}), and for higher values of the basal growth rate (higher *r*) and lower values of density-dependent mortality (lower *s*). This highlights that the local demography of killing by T6SS pushes the system towards decomposition even for fluctuations on short length scales, while higher diffusion/dispersal of cells mean that fluctuations of longer length scales are required for decomposition to occur.

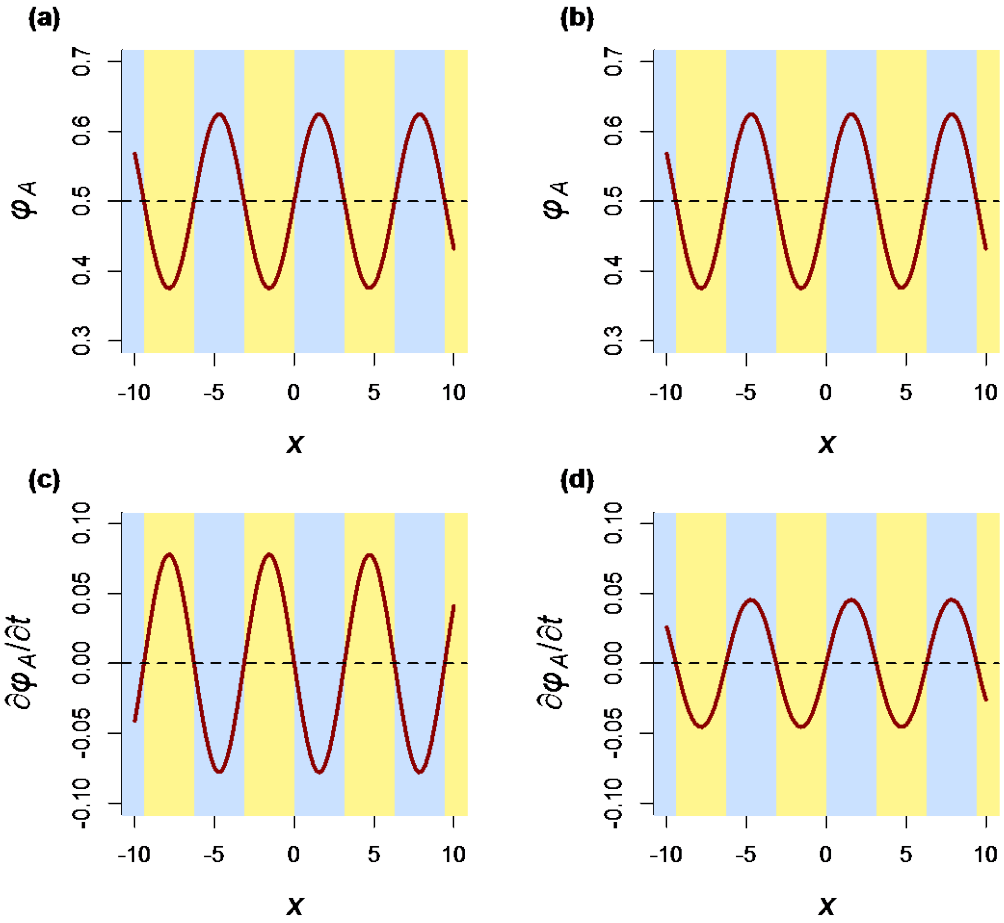

Figure SE1.2. Illustration of spatial decomposition of mixed equilibrium in one dimension. Plotted are the proportion of cells of strain *A* (φ_A) in (a) and (b), and the rate of change in this proportion ($\partial\varphi_A/\partial t$) in (c) and (d) along a spatial axis *x*. The different shaded regions indicate regions of positive (blue) and negative (yellow) fluctuation in composition. In (a) and (c) a high rate of bacterial dispersal/diffusion (*d* = 1) through space means that the fluctuation in the density of *A* is on narrow a scale relative to bacterial dispersal/diffusion and the system will return towards the spatially homogenous equilibrium ($\partial\varphi_A/\partial t$ and φ_A are of opposite sign) as bacterial/dispersal diffusion is strongly homogenising. However, in (b) and (d) when the bacterial dispersal/diffusion rate is lower (*d* = 0.01) the spatial fluctuations occur on a wider scale relative to bacterial dispersal/diffusion and the system will be begin to decompose into areas divergent in composition ($\partial\varphi_A/\partial t$ and φ_A are of opposite sign) as bacterial dispersal/diffusion is a relatively weak force compared to the demographic effects of killing. Other parameter values are *r* = 2, *s* = 2, α_{AB} = 1, α_{BA} = 1, *a* = 0.1 and β = 1.

Supplementary Equations 2. Relationship to the Allen-Cahn equation.

The Allen-Cahn equation governs the density of strains A and B during phase separation absent the conservation of strains A and B. Assuming that the *effective* diffusion rate d_{eff} doesn't vary through space (as will be approximately the case when oscillations in composition are of vanishingly small amplitude, $a \to 0$) we can write the Allen-Cahn equation for strain *A* as

$$\frac{\partial\varphi_A}{\partial t} = \Gamma\left(d\Delta\varphi_A - \frac{\partial f(\varphi_A)}{\partial\varphi_A}\right) \tag{10}$$

Where $f(\varphi_A)$ is a function of φ_A. The $\partial f(\varphi_A)/\partial\varphi_A$ term drives φ_A to the free energy minimum over time, and can work with or against diffusion. Thus, the effective diffusion is uphill whenever $\partial\varphi_A/\partial t$ and $\Delta\varphi_A$

are of opposite sign (i.e. whenever the change in volume fraction is of opposite sign to the Laplacian). The Laplacian, $\Delta\varphi_A$ is given by

$$\Delta\varphi_A = -\sin\beta x \frac{a\beta^2\left(\alpha_{AB}\alpha_{BA}K + r(\alpha_{AB}+\alpha_{BA})\right)}{(r-m)(\alpha_{AB}+\alpha_{BA})K} \tag{11}$$

The sign of $\Delta\varphi_A$ is therefore given by the sign of $-\sin\beta x$, and it follows that $\partial\varphi_A/\partial t$ and $\Delta\varphi_A$ will be of opposite sign, and effective diffusion will be uphill, in the limit of infinitesimally small amplitude fluctuations ($a \to 0$) whenever inequality 9 is satisfied. This highlights the two counteracting forces governing whether decomposition occurs – the diffusion/dispersal of cells favours downhill diffusion, while the local demographic effects of killing mimic uphill diffusion by a strain's relative growth rate being increased in regions in which it is in the majority.

Supplementary Equations 3. Adding public goods to the model.

To consider the effects of T6SS-mediated phase separation on the evolution of cooperation we extend our model so that strain *A* produces a diffusable public good secretion at rate ρ, while strain *B* does not invest in its production. We assume that strain *A* pays a growth rate cost *c* for production of the secretion. We also assume that the secretion increases each strains growth rate by amount *b* per unit concentration *S* by increasing nutrient availability (e.g. an exoenzyme digesting a substrate or siderophores binding insoluble iron). From these assumptions we write the dynamics of the two strains and the secretion concentration as

$$\frac{dA}{dt} = A(r - c + bS - s(A+B) - \alpha_{AB}B) \tag{12}$$

$$\frac{dB}{dt} = B(r + bS - s(A + B) - \alpha_{BA}A)$$

$$\frac{dS}{dt} = \rho A - \lambda S$$

for a well-mixed, non-spatial system and as

$$\frac{\partial A}{\partial t} = A(r - c + bS - s(A + B) - \alpha_{AB}B) + d\Delta A$$

$$\frac{\partial B}{\partial t} = B(r + bS - s(A + B) - \alpha_{BA}A) + d\Delta B \quad (13)$$

$$\frac{\partial S}{\partial t} = \rho A - \lambda S + D\Delta S$$

for a spatially extended system, where λ is the decay rate of the secretion, *D* is its diffusion coefficient, and all other variables are as previously defined. We numerically explore both the non-spatial and spatial systems in the presence ($\alpha_{AB} > 0,\ \alpha_{BA} > 0$) and absence ($\alpha_{AB} = 0,\ \alpha_{BA} = 0$) of killing in the main text, and here we analytically explore these four scenarios.

Non-spatial model in the absence of killing. In order to gain analytical insight into our model we will make the assumption that the dynamics of the public good occur on a much faster time-scale than the ecological dynamics so that we may treat the public good as being at equilibrium for any given ecological state of the model. For the non-spatial model this gives us

$$S = \frac{\rho A}{\lambda} \quad (14)$$

Substituting this into equation 10 and setting $\alpha_{AB} = 0,\ \alpha_{BA} = 0$ the dynamics of the two strains are

$$\frac{dA}{dt} = A\left(r - c + \frac{\rho bA}{\lambda} - s(A + B)\right) \quad (15)$$

$$\frac{dB}{dt} = B\left(r + \frac{\rho bA}{\lambda} - s(A+B)\right)$$

We will assume throughout that $s > \rho b/\lambda$, such that in the absence of cheaters a population of cooperators has a finite stable equilibrium. Solving for the equilibrium of equation 15 we can see that the only stable equilibrium is $B = r/s$ so long as $c > 0$. This means that, as long as there is a cost of cooperation, cheaters will always outcompete cooperators in a non-spatial environment in the absence of killing.

Non-spatial model with killing. Again using the assumption that public goods dynamics play out on a faster time-scale than the ecological dynamics but now setting $\alpha_{AB} = \alpha_{BA} = \alpha$ (i.e. assuming symmetric killing) the dynamics of the two strains are

$$\begin{aligned} \frac{dA}{dt} &= A\left(r - c + \frac{\rho bA}{\lambda} - s(A+B) - \alpha B\right) \\ \frac{dB}{dt} &= B\left(r + \frac{\rho bA}{\lambda} - s(A+B) - \alpha A\right) \end{aligned} \tag{16}$$

For this system there are two single strain equilibria, one for a pure population of cooperators at

$$\begin{aligned} A &= \frac{\lambda(r-c)}{\lambda s - \rho b} \\ B &= 0 \end{aligned} \tag{17}$$

and one for a pure population of cheaters at

$$\begin{aligned} A &= 0 \\ B &= \frac{r}{s} \end{aligned} \tag{18}$$

The cooperator equilibrium is stable so long as $\alpha > c(\lambda s - \rho b)/(\lambda r - \lambda c)$, while the cheater equilibrium is always stable. There is a an unstable saddle point at

$$A = \frac{\lambda(\alpha r + cs)}{\alpha(\alpha\lambda + 2\lambda s - \rho b)}$$
$$B = \frac{\alpha\lambda r + \rho bc - c(\alpha + s)}{\alpha(\alpha\lambda + 2\lambda s - \rho b)} \quad (19)$$

which exists whenever $\alpha > c(\lambda s - \rho b)/(\lambda r - \lambda c)$. This means that in the presence of killing cooperation can potentially still be a stable outcome. However, the location of the saddle point given is always at a higher value of *A* than of *B* (i.e. *A* is always larger than *B* in equation 19 whenever *c* > 0), meaning that the basin of attraction for strain *A* is smaller than that for strain *B*. Thus, though killing can help protect cooperation from cheaters in a non-spatial environment, they are still disfavoured compared to cheaters. More generally, the condition for the cooperative strain to increase in frequency is

$$\alpha(A - B) > c \quad (20)$$

Here we see that, in a non-spatial environment killing can help protect cooperators owing to the positive frequency dependence that it induces. However, cooperators are still disfavoured compared to cheaters as the basin of attraction for cheaters is larger (equation 19).

***Spatial model in the absence of killing*.** We will consider a one-dimensional spatial environment with a fluctuation in the strain composition as given in equation 5. Using this spatial distribution of strains and assuming that the public goods dynamics happen on a much faster timescale than the ecological dynamics, we can solve for the equilibrium concentration of the public good across space as

$$S(x) = \frac{\rho A_0}{\lambda} + \frac{\rho a \sin \beta x}{\beta^2 D + \lambda} \quad (21)$$

Note here that as the diffusion rate of the public good approaches infinity ($D \to \infty$) this simplifies to $S(x) = \rho A_0/\lambda$, and thus has a constant concentration through space, while as the diffusion rate of the public good approaches zero it simplifies to $S(x) = \rho(A_0 + a \sin \beta x)/\lambda$, and is thus simply proportional

to the local density of the cooperator strain. Using equations 11 and 18 and setting $\alpha_{AB} = \alpha_{BA} = 0$ we get

$$\frac{\partial A}{\partial t} = (A_0 + a\sin\beta x)\left(r - c - s(A_0 + B_0) + \frac{\rho b A_0}{\lambda} + \frac{\rho b a \sin\beta x}{\beta^2 D + \lambda}\right) - \beta^2 a d \sin\beta x$$
$$\frac{\partial B}{\partial t} = (B_0 - a\sin\beta x)\left(r - s(A_0 + B_0) + \frac{\rho b A_0}{\lambda} + \frac{\rho b a \sin\beta x}{\beta^2 D + \lambda}\right) + \beta^2 a d \sin\beta x \quad (22)$$

We can evaluate the fitness (per cell growth rate) of each strain as

$$w_A = \frac{\int {}^{\partial A}/_{\partial t}\, \mathrm{d}x}{\int A\, \mathrm{d}x}$$
$$w_B = \frac{\int {}^{\partial B}/_{\partial t}\, \mathrm{d}x}{\int B\, \mathrm{d}x} \quad (23)$$

We can then evaluate when cooperators are favoured by evaluating the inequality $w_A > w_B$, which gives

$$\frac{\rho a^2 b(A_0 + B_0)}{2A_0 B_0(\beta^2 D + \lambda)} > c \quad (24)$$

as the condition for cooperators to increase in frequency. This condition is more easily favoured for lower costs of cooperation (low *c*), higher benefits of cooperation (high *b*), and with spatial fluctuations that are of large amplitude (high *a*) and over a wide spatial scale (low β).

Inequality 24 shows that cooperation can be favoured by spatial variance in the population composition. However, in the absence of outside forces or stochastic effects will such spatial fluctuations be maintained? To answer this we first evaluate an expression for the change in the density/volume fraction of the cooperator strain giving

$$\frac{\partial \varphi_A}{\partial t} = -\frac{cA_0B_0 - a\sin\beta x\,(c(A_0 - B_0) - \beta^2 d(A_0 + B_0) + ac\sin\beta x)}{(A_0 + B_0)^2} \quad (25)$$

which is always negative, meaning that the cooperator strain is always locally decreasing in frequency, even when globally increasing in frequency. This means that the change in cooperator frequency cannot match the sign of the spatial fluctuation $\Delta\varphi_A$, and thus in the absence of external forces any spatial fluctuations in composition will be lost. As we can see from inequality 24 as the amplitude of the fluctuation decays to zero (a approaches 0) cooperation cannot be favoured, and thus without killing, external perturbations to the system or stochastic effects are required to maintain the spatial structure necessary to maintain cooperation.

Spatial model with killing. We now set $\alpha_{AB} = \alpha_{BA} = \alpha > 0$ and evaluate the consequences of the combination of killing and a spatial environment of the dynamics of cooperation. From our assumptions the dynamics are now given by

$$\begin{aligned}\frac{\partial A}{\partial t} &= (A_0 + a\sin\beta x)\left(r - c - s(A_0 + B_0) - \alpha(B_0 - a\sin\beta x) + \frac{\rho b A_0}{\lambda}\right. \\ &\quad \left. + \frac{\rho b a \sin\beta x}{\beta^2 D + \lambda}\right) - \beta^2 a d \sin\beta x \\ \frac{\partial B}{\partial t} &= (B_0 - a\sin\beta x)\left(r - s(A_0 + B_0) - \alpha(A_0 + a\sin\beta x) + \frac{\rho b A_0}{\lambda} + \frac{\rho b a \sin\beta x}{\beta^2 D + \lambda}\right) \\ &\quad + \beta^2 a d \sin\beta x\end{aligned} \tag{26}$$

We can again evaluate the fitness of each strain as in equation 23, and derive the condition for the cooperative strain to be favoured ($w_A > w_B$) as

$$\frac{\rho a^2 b(A_0 + B_0)}{2A_0B_0(\beta^2 D + \lambda)} + \frac{\alpha(A_0 - B_0)(2A_0B_0 - a^2)}{2A_0B_0} > c \tag{27}$$

Note that if the cooperator and cheater strains are at equal average density ($A_0 = B_0$) this simplifies to the inequality given in 24. As the amplitude of the spatial fluctuation must be less than the average density of the less abundant of the two strains ($a < \min\{A_0, B_0\}$) the condition given in inequality 27 is more easily satisfied than that in inequality 24 whenever $A_0 > B_0$ and less easily satisfied whenever $A_0 < B_0$.

This occurs owing to the positive frequency dependence introduced by killing. However, as we will show, unlike in a spatial environment without killing, killing in a spatial environment can increase structuring, thus further favouring cooperation.

Comparing inequality 27 (condition for cooperation to increase in frequency in a spatial environment with killing) with inequality 20 (condition for cooperation to increase in frequency in a non-spatial environment with killing), we can also see that the presence of spatial heterogeneity means that the cooperator can be favoured even when numerically less abundant in a spatial environment with killing (i.e. inequality 27 can be satisfied when inequality 20 is not). This occurs as spatial heterogeneity can allow cooperators to disproportionately gain the benefits of cooperation compared to cheaters.

Finally, we will show that killing causes phase separation in a spatial environment when one strain is a cooperator and the other a cheat. We follow the same approach as before and consider whether a spatial fluctuation around the homogenous coexistence equilibrium given in equation 17 will be amplified, which can be evaluated by considering if $\partial\varphi_A/\partial t$ has the same sign as the fluctuation $\sin\beta x$. At any point of zero compositional fluctuation ($x = n\pi/\beta$, where $n \in \mathbb{Z}$), $\partial\varphi_A/\partial t = 0$ and this condition cannot be fulfilled. However, the condition for $\partial\varphi_A/\partial t$ and $\sin\beta x$ to have the same sign in a region of non-zero fluctuation ($x \neq n\pi/\beta$, where $n \in \mathbb{Z}$) in the limit of an infinitesimally small amplitude for the compositional fluctuation ($a \to 0$) is

$$\frac{2\lambda(\alpha r + cs)(\alpha\lambda r - c(\alpha + s) + \rho bc)}{(\alpha\lambda(2r - c) + \rho bc)(\alpha\lambda + 2\lambda s - \rho b)} > d\beta^2 \qquad (28)$$

This shows that killing promotes phase separation of cooperator and cheater strains in a spatial environment which favours cooperators of cheats as shown in inequality 27.

Taken together, these results show that:

(1) Killing in a non-spatial environment can protect cooperators from cheats when the cooperator is at higher abundance. However, cooperators cannot invade from rarity.

(2) Heterogeneity in a spatial environment without killing can favour cooperators over cheats. However, in the absence of any external forces or stochastic effects (e.g. bottlenecking during range expansion) this structure will ultimately be lost, allowing cheaters to win.

(3) In a spatial environment with killing phase separation can occur, protecting cooperators from cheats and potentially allowing them to invade from rarity.

References

1 Bernardy, E. E., Turnsek, M. A., Wilson, S. K., Tarr, C. L. & Hammer, B. K. Diversity of Clinical and Environmental Isolates of Vibrio cholerae in Natural Transformation and Contact-Dependent Bacterial Killing Indicative of Type VI Secretion System Activity. *Applied and environmental microbiology* **82**, 2833-2842 (2016).